SPANDIDOS PUBLICATIONS

EXPERIMENTAL AND THERAPEUTIC MEDICINE 17: 1282-1289, 2019

Gemfibrozil reduces lipid accumulation in SMMC-7721 cells via the involvement of PPARα and SREBP1

XIAONAN ZHANG, SONG WANG, LINLIN HU, JIAN WANG, YAJING LIU and PING SHI

State Key Laboratory of Bioreactor Engineering, East China University of Science and Technology, Shanghai 200237, P.R. China

Received September 4, 2016; Accepted November 12, 2018

DOI: 10.3892/etm.2018.7046

Abstract. Gemfibrozil (GEM) is a member of the fibrate class of lipid-lowering pharmaceuticals and has been widely used in the therapy of different forms of hyperlipidemia and hypercholesterolemia. Non-alcoholic fatty liver disease (NAFLD) is the most common chronic liver disease and is becoming an important public health concern worldwide. However, there is little knowledge about the effects of GEM on NAFLD. In the present study, oleate-treated human hepatoma SMMC-7721 cells were utilized to investigate the role of GEM in regulating hepatic lipid metabolism. The present results demonstrated that GEM attenuated excessive intracellular triglyceride content in the steatosis model. Upregulation of peroxisome proliferator-activated receptor α (PPARα) protein and sterol regulatory element-binding protein 1 (SREBP1) was detected following treatment with GEM. Additionally, reverse transcription-polymerase chain reaction analysis demonstrated that GEM increased the downstream genes related to PPARα and SREBP1, including carnitine palmitoyltransferase 2, acyl-coA oxidase 1, hydroxyacyl-CoA dehydrogenase, LIPIN1 and diacylglycerol O-acyltransferase 1. These findings demonstrated that GEM alleviated hepatic steatosis via the involvement of the PPARα and SREBP1 signaling pathways, which enhances lipid oxidation and interferes with lipid synthesis and secretion. Taken together, the data provide direct evidence that GEM may lower lipid accumulation in hepatocellular steatosis cells *in vitro* and that it may have a potential therapeutic use for NAFLD.

Introduction

Gemfibrozil (GEM) is a member of the fibrate class of lipid-lowering pharmaceuticals and has been widely used in the therapy of different forms of hyperlipidemia and hypercholesterolemia since the early 1970s (1). Fibrates act as agonists of the nuclear receptor peroxisome proliferator-activated receptor α (PPARα), which regulates gene expression for lipid catabolism and lipoprotein metabolism (2). Fibrates cause a moderate decrease in the content of plasma triglycerides (TG) and increase cholesterol level in high density lipoproteins (3). Clinical trials have demonstrated that fibrates have a benignant effect on vascular remodeling, inflammation, cardiovascular and coronary events (4,5). However, there is currently little understanding about the effects on fatty liver disease after drug treatment, particularly in hepatocytes.

Non-alcoholic fatty liver disease (NAFLD) includes a broad spectrum of liver injury, which is characterized by fat infiltration (steatosis) with a TG content >5% liver weight with no alcohol consumption, which is different from alcoholic fatty liver disease (6). NAFLD has been correlated with obesity, diabetes, insulin resistance, hypertriglyceridemia and cardiovascular diseases, and represents the hepatic manifestation of the metabolic syndrome (7-9). Furthermore, the development process of liver disease includes several stages, ranging from regional steatosis to nonalcoholic steatohepatitis, and even to serious liver disease, such as cirrhosis and hepatocellular carcinoma (10). It was estimated that the prevalence of NAFLD ranges from 17-33% in the general population of Western countries in 2003 (11). Unfortunately, current effective therapies for NAFLD are limited and therefore there is a critical requirement to identify the mechanisms of NAFLD. According to the two-hit theory, the hallmark of NAFLD is triacylglycerol accumulation in lipid droplets within hepatocytes (12,13). In the present study, oleate-treated human hepatoma SMMC-7721 cells were utilized as a model of steatosis (14,15) to investigate the role of GEM in regulating hepatic lipid metabolism.

Materials and methods

Antibodies and reagents. Cluster of differentiation (CD)36, sterol regulatory element-binding protein 1 (SREBP1) and PPARα antibodies were separately purchased from Santa Cruz Biotechnology, Inc., (Dallas, TX, USA). β-actin rabbit monoclonal antibody was purchased from Abcam (Cambridge, MA, USA). Secondary horseradish peroxidase-labeled goat anti-rabbit immunoglobulin G (H+L) was purchased from

Correspondence to: Professor Ping Shi, State Key Laboratory of Bioreactor Engineering, East China University of Science and Technology, 130 Meilong Road, Shanghai 200237, P.R. China
E-mail: ship@ecust.edu.cn

Key words: human hepatoma SMMC-7721 cells, oleic acid, gemfibrozil

Novoprotein Scientific, Inc. (Summit, NJ, USA). GEM was purchased from Sigma-Aldrich (Merck KGaA, Darmstadt, Germany). Oleic acid (OA) and bovine serum albumin (BSA; fatty acid free) were obtained from Sangon Biotech Co., Ltd., (Shanghai, China).

Cell culture and treatment. Human hepatoma SMMC-7721 cells were supplied by the Institute of Cell Biology (Shanghai, China). The cells were cultured in RPMI-1640 medium (Gibco; Thermo Fisher Scientific, Inc., Waltham, MA, USA) supplemented with 10% fetal bovine serum (Biological Industry, Kibbutz Beit Haemek, Israel), 1% penicillin-streptomycin (10,000 U/ml penicillin and 10 mg/ml streptomycin; Beijing Solarbio Science & Technology Co., Ltd., Beijing, China) and maintained at 37˚C with humidified air in 5% CO_2. SMMC-7721 cells were first exposed to GEM when they reached 75% confluence. Different dilutions (10-200 μM) of GEM were made with DMSO and 10 μl of GEM solutions were then added to 1 ml culture medium, respectively. To investigate the effect of OA on fat-overloading, cultures were exposed to different concentrations of OA, diluted in 10% BSA, ranging from 0.5-2 mM.

Cell viability assay. To determine the effect of GEM or OA on SMMC-7721 cell viability, the cells were treated with GEM at different concentrations (0, 50, 100 and 200 μM) for 24 and 48 h at 37˚C. Following this, $1x10^6$ cells in 96-well plates were treated with OA at different concentrations (0, 0.5, 1, 1.5 and 2 mM) with 10% BSA overnight at 37˚C, respectively. Cell viability was determined using Cell Counting kit-8 dye (Beyotime Institute of Biotechnology, Beijing, China), according to manufacturer's instructions. Absorbance was measured at 450 nm with a GENios multifunction-reader (Tecan GENios Pro; Tecan Group, Ltd., Männedorf, Switzerland).

Evaluation and quantification of lipid accumulation. Oil red O (Sangon Biotech Co. Ltd., Shanghai, China) was used to monitor the content of lipids in SMMC-7721 cells, according to the manufacturer's instructions. Cells were seeded in a 6-well plate at a density of $1.0x10^5$ cells/well. Following adherence, cells were treated with GEM at different concentrations (0, 10, 25, 50 and 100 μM) together with 1 mM OA for 24 h at 37˚C, respectively. Subsequently, cells were fixed overnight at 37˚C with 4% paraformaldehyde and stained with Oil red O at 37˚C for 30 min. Images were photographed with an inverted fluorescent microscope (Nikon Eclipse TI; Nikon Corp., Tokyo, Japan). Following this, Oil red O was extracted using isopropanol (100 μl) for 1 h at 37˚C. Then the extracted sample was moved to another 96-well plate. Absorbance was measured at 510 nm in a spectrophotometer for quantitative analysis (16).

Extraction and quantification of TG. For quantitative estimation of TG, lipids were extracted from cells using Triton X-100 (2%) for 30 min at 37˚C. An enzymatic assay was then performed using an EnzyChromTM Triglyceride Assay kit (Bioassay Systems LLC, Hayward, CA, USA), according to the manufacturer's protocols. Total lipid extraction and separation was conducted by thin layer chromatography (TLC), according to previous methods (16). The cell pellets were harvested by centrifugation at 1,000 x g for 5 min at 37˚C, washed twice with phosphate-buffered saline (PBS), snap-frozen and smashed in 1 ml methanol chloroform mix (v/v, 2/1). These components were mixed well and then centrifuged at 12,000 x g for 5 min at room temperature to allow phase separation. The chloroform phase was transferred to a new tube and blow-dried. The lipid fractions were separated by TLC using a developing solvent (hexane/diethyl ether/acetic acid; 40:80:2, v/v/v). To visualize different fractions of total lipids extracted from cells, the TLC plate (Sinopharm Chemical Reagent Co., Ltd., Beijing, China) was stained with iodine vapor at 60˚C for 30 min and photographed using a DNR Bio-Imaging System, Ltd. (Neve Yamin, Israel).

RNA isolation, reverse transcription-polymerase chain reaction (RT-PCR) and RT-quantitative PCR (RT-qPCR) analyses. Total RNA was extracted using RNAiso Plus (Takara Biotechnology Co. Ltd., Dalian, China), according to the manufacturer's instructions, and quantified using a NanoDrop 2000c (Thermo Fisher Scientific Inc., Waltham, MA, USA). First-strand cDNA synthesis (1 μg) and PCR reactions were performed using the PrimeScriptTM RT reagent kit with gDNA Eraser (Takara Biotechnology Co. Ltd., Dalian, China), according to the manufacturer's instructions. Following this, mRNA levels were determined by PCR (EmeraldAmp PCR MasterMix; Catalogue no. RR300A; Takara Biotechnology Co. Ltd., Dalian, China), as described in the study by Bergman *et al* (17). The primers were designed using Primer 5.0 software (Premier Biosoft International, Palo Alto, CA, USA) and are listed in Table I. 18S ribosomal (r) RNA was selected as an internal control. The PCR reaction conditions were as follows: 98˚C for 10 sec, 55˚C for 30 sec and 72˚C for 1 min for a total 30 cycles. qPCR was performed in triplicate assays using SYBR Premix Ex Taq (Tli RNaseH Plus; catalogue no. RR420; Takara Biotechnology Co. Ltd., Dalian, China) in a CFX96 Real-Time PCR Detection System (Bio-Rad Laboratories, Inc., Hercules, CA, USA). The qPCR reaction conditions were as follows: Activation of the Taq DNA polymerase at 95˚C for 30 sec, followed by 40 cycles of 95˚C for 10 sec and 60˚C for 32 sec. mRNA expression levels were analyzed by the $2^{-\Delta\Delta Cq}$ method (18), relative to 18S rRNA expression.

Western blotting. Cells were incubated with either OA (1 mM) or OA together with GEM (50 μM) for 24 h at 37˚C and lysed with pre-chilled radioimmunoprecipitation assay lysis buffer (Beyotime Institute of Biotechnology) for 30 min on ice. Following this, lysates were centrifuged at 13,000 x g for 20 min at 4˚C and quantified by a Bradford protein assay (Bio-Rad Laboratories, Inc.) (19). Proteins (50 μg) were separated by 8% SDS-PAGE and transferred to Amersham Hybond-P polyvinylidene fluoride membranes (GE Healthcare Life Sciences, Little Chalfont, UK). Membranes were blocked with 5% milk powder in PBS for 2 h at 37˚C and then incubated with primary specific antibodies overnight at 4˚C, including CD36 (catalogue no. sc-9154; 1:2,000), PPARα (catalogue no. sc-9000; 1:1,000), SREBP1 (catalogue no. sc-8984; 1:1,000) and β-actin (catalogue no. ab8226; 1:5,000) rabbit monoclonal antibodies. The membrane was placed in

Table I. Sequences of primers used in the present study.

	Primer sequence (5'-3')	
Gene	Forward	Reverse
CD36	GAGAACTGTTATGGGGCTAT	TTCAACTGGAGAGGCAAAGG
PPARα	GCGATCTAGAGAGCCCGTTATC	GCCAAAGCTTCCAGAACTATCC
SREBP1	CTGGTCGTAGATGCGGAGAA	CATTGATGGAGGAGCGGTAG
LIPIN1	GACCTCACAGACATGGATCCTGAAG	ACCGGGCTCCGTTGTCGCTTGCATG
LIPIN2	AACAAGTCATCGTATCACAGG	CTCGCCAGTAGCAGAAGG
DGAT1	GCAGCCTCTTTCCTTCACTT	GACCTCCCGCTACCATCAA
DGAT2	CGAAAGCCACTTCTCATACA	TGCCTACTACTGCCCTCAC
CPT1	AAATTACGTGAGCGACTGG	CTGCCTGAATGTGAGTTGGA
CPT2	CTGGTCAATGCGTATCCC	GCCCAGATGTCTCGGTTC
ACOX1	GAAACCGCTGAGTAACAA	ACAAACTGGAAGGCATAG
HADHA	GGGATGTGGCAGTTGTTC	GGACGGCACTTCTGATTT
18S rRNA	CGGCTACCACATCCAAGGAAG	AGCTGGAATTACCGCGGCT

PBS-Tween 20 (PBST) and cleaned 3 times for 10 min. Then samples were incubated with secondary horseradish peroxidase (HRP)-labeled goat anti-rabbit immunoglobulin G (H+L) (catalogue no. L153B; 1:1,000) at room temperature for 1.5 h. After completion of secondary antibody incubation, wash 3 times in PBST for 10 min/time Target proteins on the membranes were visualized using Pro-light HRP Chemiluminescent kit (cat. no. PA112; Tiangen Biotech Co., Ltd., Beijing, China) following the manufacturers protocol. The protein bands were analyzed by densitometry using ImageJ software, version 1.37 (National Institutes of Health, Bethesda, MD, USA) after exposure of the membranes to gel capture software, version 2.0 (DNR Bio-Imaging System, Ltd., Jerusalem, Israel).

Statistical analysis. All experiments were performed at least three times. Values were expressed as the mean ± standard deviation. Statistical analysis was performed using the Student's t-test using SPSS version 19.0 (IBM Corp., Armonk, NY, USA). P<0.05 was considered to indicate a statistically significant difference.

Results

Cytotoxicity of GEM in an in vitro hepatocellular model. Using the WST-8 based Colorimetric Assay Cell Counting kit-8, the effect of GEM on cell viability was measured. As demonstrated in Fig. 1A, no significant cytotoxic effect was observed in cells following treatment with GEM. Cell viability of SMMC-7721 cells was inhibited by 4.22, 9.72 and 9.55% at GEM concentrations of 50, 100 and 200 μM after 24 h, respectively. Cells were also exposed to different concentration of OA. The concentrations of OA were chosen according to our previous work (15). As demonstrated in Fig. 1B, OA inhibited cell viability in a dose- and time-dependent manner. When cells were cultured in the presence of OA at 0.5 and 1 mM for 24 h, they accumulated intracellular lipids without acute cytotoxic effect, while cell viability was significantly inhibited when treated with 1.5 and 2 mM OA for 24 and

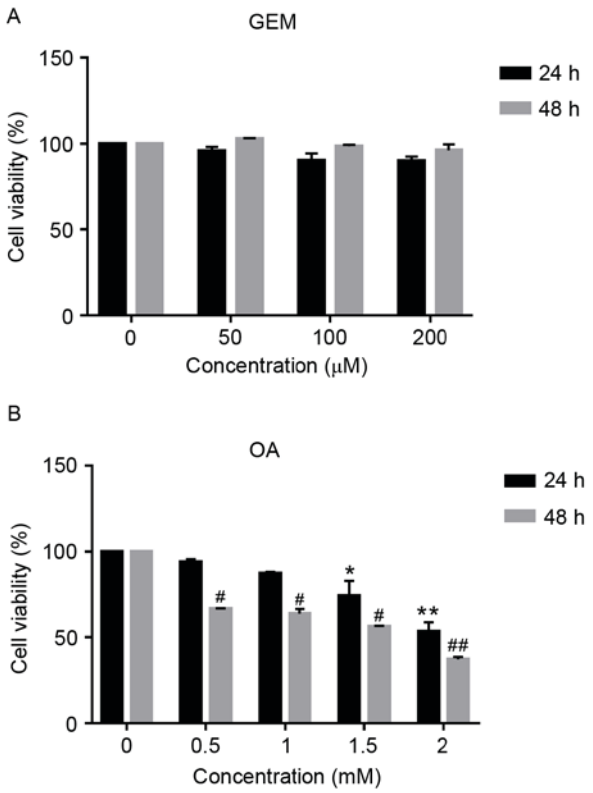

Figure 1. Effects of GEM and OA on cell viability in SMMC-7721 cells. (A) Cells were treated with GEM at different concentrations (0, 50, 100 and 200 μM) for 24 and 48 h and the effects on growth inhibition were concentration- and time-dependent. (B) Cells in 96-well plates were treated with OA at different concentrations (0, 0.5, 1, 1.5 and 2 mM) with 10% bovine serum albumin for 24 and 48 h and the effects on growth inhibition were concentration- and time-dependent. Data are presented as the mean + standard deviation of three independent experiments. *P<0.05 and **P<0.01 vs. 0 mM at 24 h. $^{\#}$P<0.05 and $^{\#\#}$P<0.01 vs. 0 mM at 48 h. GEM, gemfibrozil; OA, oleic acid.

48 h compared with 0 mM OA (P<0.05). Cell viability was decreased by 25.7 and 46.9% at 1.5 mM OA for 24 and 48 h, respectively and 44 and 62.9% at 2 mM OA for 24 and 48 h,

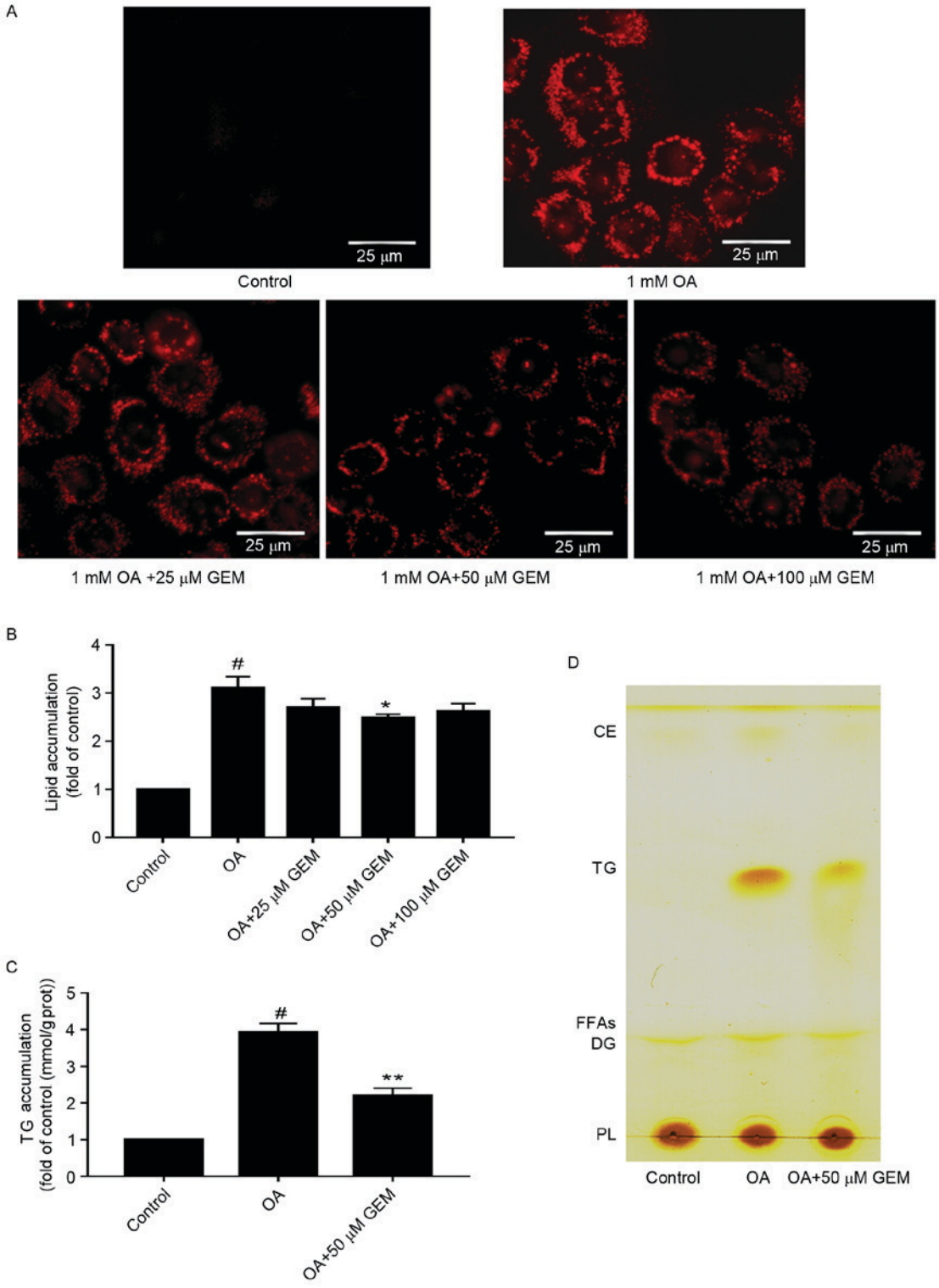

Figure 2. Effect of GEM on lipid accumulation. (A) After cells were treated with GEM at various concentrations (25, 50 and 100 μM) and 1 mM OA for 24 h, intracellular lipid droplets were stained with Oil red O and photographed by microscopy (magnification, x400; scale bar, 25 μm). (B) Quantification of lipid content in OA-overloaded cells following treatment with various concentrations (25, 50 and 100 μM) of GEM. Lipid content was expressed as the fold of control. (C) Quantification of TG content in OA-overloaded cells following treatment with 50 μM GEM. TG content was expressed as the fold of control. (D) Total lipid extraction and separation by thin layer chromatography. Data are expressed at the mean + standard deviation. $^{\#}$P<0.05 vs. control cells; *P<0.05 and **P<0.01 vs. OA only. GEM, gemfibrozil; OA, oleic acid; TG, triglyceride; CE, cholesteryl ester; FFAs, free fat acid; DG, diacylglycerol; PL, phospholipid.

respectively. Therefore, cells treated with 1 mM OA were used as the cellular model of NAFLD.

GEM ameliorates lipid accumulation. To determine whether GEM affects lipid accumulation in SMMC-7721 cells, cells were incubated with different concentrations of GEM and 1 mM OA. As demonstrated in Fig. 2A, a clear dose-dependent decrease in lipid accumulation was observed in the cells under the microscope. Furthermore, the total lipid levels were decreased by 12.9, 21 and 16.5% in cells incubated with GEM

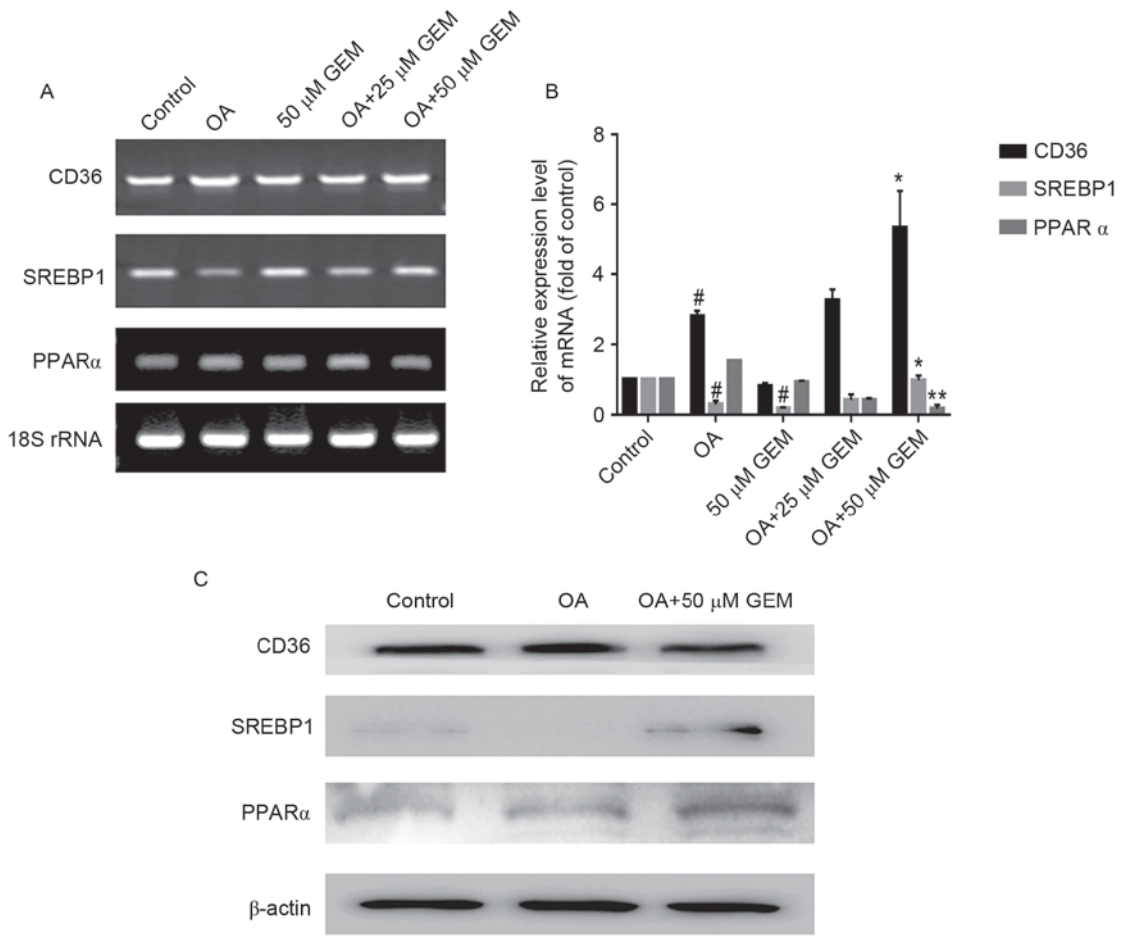

Figure 3. Effect of GEM on lipid metabolism-related gene and protein expression. (A) Reverse transcription-polymerase chain reaction results of the effect of GEM on mRNA expression levels of related genes. Cells were treated with 25 and 50 μM GEM concentrations for 24 h. (B) Reverse transcription-quantitative polymerase chain reaction analyses of effect of GEM on mRNA expression levels of related genes. (C) Effect of GEM on the expression level of CD36, PPARα and SREBP1 in SMMC-7721 cells by western blotting. β-actin was used as the loading control. The data are presented as the mean + standard deviation of three independent experiments. $^{\#}$P<0.05 vs. control cells; *P<0.05 and **P<0.01 vs. OA only. GEM, gemfibrozil; OA, oleic acid; CD, cluster of differentiation; SREBP1, sterol regulatory element-binding protein 1; PPARα, peroxisome proliferator-activated receptor α; rRNA, ribosomal RNA.

concentrations of 25, 50 and 100 μM, respectively (Fig. 2B). The results indicated that 50 μM of GEM significantly reduced levels of intracellular total lipids and TG compared with cells treated with 1 mM OA only (P<0.05; Fig. 2B and C). Therefore 50 μM was used for subsequent experiments and assessments. The level of cellular TG was detected and was observed to be decreased by 43.8% at 50 μM GEM compared with cells treated with 1 mM OA only (Fig. 2C). To further confirm the lipid changes in the cellular model, TLC analysis was performed. TLC results suggested that there was a decrease in TG levels in cells treated with 50 μM GEM compared with those treated with OA only (Fig. 2D). Taken together, GEM may lower the lipid accumulation in an *in vitro* model of NAFLD. The optimal concentration is 50 μM.

Changes to lipid metabolism-related mRNA and protein expression. RT-PCR and RT-qPCR analyses were employed to determine whether GEM was able to regulate lipid metabolism-related gene expression in SMMC-7721 cells. The results demonstrated that GEM (50 μM) significantly increased the levels of CD36, SREBP1 (P<0.05) and significantly reduced the levels of PPARα (P<0.01) in cells treated with 1 mM OA compared with cells treated with OA only (Fig. 3A and B). Subsequently, western blotting with specific antibodies was performed to detect the changes of related protein expression levels. The expression levels of SREBP1 and PPARα were markedly upregulated following treatment with GEM in the OA-overloaded cells. However, the level of CD36 in OA-overloaded cells treated with GEM showed no marked change compared with cells treated with OA only (Fig. 3C).

Confirmation of modulation of lipid synthesis and lipid oxidation. It is well recognized that lipogenic genes are commonly trans-activated by SREBP1, and this has critical central roles in the regulation of lipid synthesis (20). To validate the upregulation of SREBP1, the expression levels of its downstream target genes, such as *LIPIN1*, *LIPIN2*, *diacylglycerol O-acyltransferase (DGAT)1* and *DGAT2*, were examined in the cells. The results demonstrated that mRNA levels of *LIPIN1* and *DGAT1* were markedly increased following treatment with GEM in cells treated with OA. However, mRNA expression levels of *LIPIN2* and *DGAT2* remained unchanged (Fig. 4A). As a transcription factor, PPARα has central roles in hepatic lipid oxidation, predominantly through regulating lipid target genes, such as *carnitine palmitoyltransferase (CPT)1, CPT2, acyl-coA oxidase 1 (ACOX1)* and *hydroxyacyl-CoA*

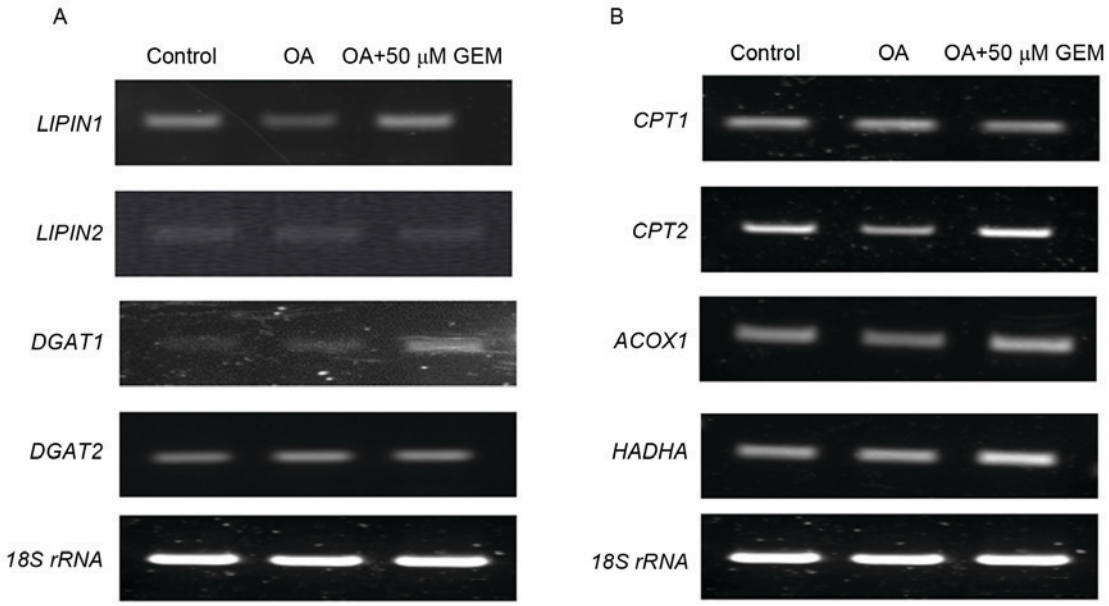

Figure 4. Effect of GEM on sterol regulatory element-binding protein 1 and peroxisome proliferator-activated receptor α targets under the same experimental conditions. (A) RT-PCR results of the effect of GEM on mRNA expression levels of *LIPIN1, LIPIN2, DGAT1* and *DGAT2*. (B) RT-PCR results of effect of GEM on mRNA expression levels of *CPT1, CPT2, ACOX1* and *HADHA*. RT-PCR, reverse transcription-polymerase chain reaction; GEM, gemfibrozil; OA, oleic acid; rRNA, ribosomal RNA; DGAT, diacylglycerol O-acyltransferase; CPT, carnitine palmitoyltransferase; ACOX1, acyl-coA oxidase 1; HADHA, hydroxyacyl-CoA dehydrogenase.

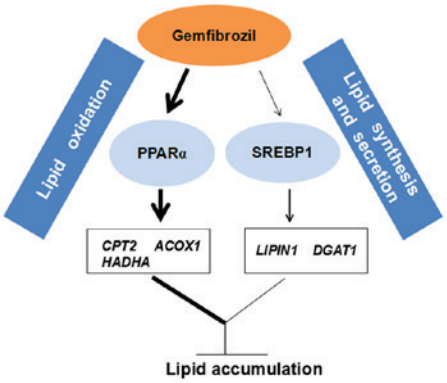

Figure 5. Schematic of the effect of gemfibrozil on lipid metabolism in an *in vitro* hepatocellular steatosis cell model. SREBP1, sterol regulatory element-binding protein 1; PPARα, peroxisome proliferator-activated receptor α; CPT, carnitine palmitoyltransferase; ACOX1, acyl-coA oxidase 1; DGAT, diacylglycerol O-acyltransferase; HADHA, hydroxyacyl-CoA dehydrogenase.

dehydrogenase (HADHA) (21,22). Therefore, mRNA expression level changes of these genes were measured. The data demonstrated that mRNA levels of *CPT2, ACOX1* and *HADHA* were significantly increased in the cellular model of NAFLD treated with GEM compared with the OA control, while the *CPT1* mRNA expression level was not altered (Fig. 4B). Therefore, GEM may lower TG accumulation in OA-overloaded SMMC-7721 cells via the involvement of the PPARα and SREBP1 signaling pathways (Fig. 5).

Discussion

Previous studies have demonstrated that GEM functions as a PPARα agonist and is employed to treat hyperlipidemia and hypercholesterolemia (1,2,4). A study by Smith *et al* (23) reported that large significant declines in TG and smaller but significant declines in total lipids were the classical response to GEM treatment in patients with hypertriglyceridemia. In our laboratory, an *in vitro* hepatocellular steatosis model has been successfully established in human SMMC-7721 cells by using OA (15). In the present paper, the effect of GEM on this cellular model was examined. The present results demonstrated that GEM affected the expression levels of genes and proteins related to lipid metabolism, leading to a decrease in the lipid content and TG level in the fat over-accumulating hepatocytes.

PPARα belongs to the nuclear receptor family and is responsible for the regulation of lipid metabolism (24). The roles of PPARα in hepatic lipid homeostasis are well established, it governs β-oxidation to decrease lipid storage (25). PPARα agonist treatment protects wild type mice fed a methionine choline deficient (MCD) diet from both steatosis and steatohepatitis by preventing hepatic lipid accumulation (26). The results of the present study demonstrated that mRNA and protein levels of PPARα were altered in OA-overloaded SMMC-7721 cells treated with GEM, which was consistent with an increase in the expression levels of CPT2, ACOX1 and HADHA. A study by Ogata *et al* (27) observed the increase of hepatic lipid oxidation in rats on a high fat diet supplemented with GEM. GEM increased mRNA abundance of PPARα, as well as several of its downstream targets in the male goldfish and zebrafish (28,29). In the current study, the mRNA expression levels of *PPARα* decreased while the protein expression of PPARα was increased following treatment with GEM. Therefore, the present results demonstrated further that GEM functions as a PPARα agonist to activate lipid oxidation, leading to the reduction of excessive intracellular TG content in the hepatic steatosis model.

In addition, the present study indicated that GEM induced an increase in the mRNA and protein levels of SREBP1, accompanied by an increase in *LIPIN1* and *DGAT*1 mRNA. SREBP1 is an important regulator of various genes involved in hepatic lipid metabolism and homeostasis (30). SREBP1 is a transcription factor that controls the anabolic pathways of cholesterol, free fat acids (FFAs) and TG (31). In FFA metabolism, SREBP-1 upregulates the expression of *de novo* lipogenesis via fatty acid synthase (32). Elevated SREBP-1c increases lipogenic gene expression, enhances fatty acid synthesis and accelerates TG accumulation in mice (33). As one of the downstream target genes of SREBP-1, LIPIN1 has been reported to encode significant hepatic phosphatidic acid phosphatase (PAP) activity (34). LIPIN1 deficiency is associated with lipodystrophy and hepatic steatosis in mice (35). DGAT activities catalyze the synthesis of TG in lipid droplets for storage or in nascent lipoproteins for secretion (36). Additionally, inhibition of DGAT1 increased triacylglycerol secretion, while inactivation of DGAT1 promoted large lipid droplet formation (37). From the present results, it is evident that GEM is involved in TG synthesis and secretion.

CD36 is a membrane-associated protein that facilitates the uptake of chylomicron and very low density lipoprotein remnants, as well as long-chain FFAs (38,39). Elevated CD36 expression is involved in steatosis of animal models (40,41). In patients with NAFLD and chronic hepatitis C virus, upregulation of CD36 expression is also detected (42). However, it appeared that the expression of CD36 was not affected by GEM in the present *in vitro* model.

In conclusion, GEM lowers TG accumulation in OA-overloaded SMMC-7721 cells via the involvement of the PPARα and SREBP1 signaling pathways, which enhances lipid oxidation and interferes with lipid synthesis and secretion. The present results strongly suggest that GEM may potentially be utilized for the treatment of NAFLD.

Acknowledgements

The present work was sponsored by grants from Shanghai Scientific and Technological Innovation Project (grant no. 14520720700) and State Education Ministry and Fundamental Research Funds for the Central Universities (grant no. 222201313010).

Competing interests

The authors declare that they have no competing interests.

References

1. Fruchart JC and Duriez P: Mode of action of fibrates in the regulation of triglyceride and HDL-cholesterol metabolism. Drugs Today (Barc) 42: 39-64, 2006.
2. Mandard S, Müller M and Kersten S: Peroxisome proliferator-activated receptor alpha target genes. Cell Mol Life Sci 61: 393-416, 2004.
3. Chinetti-Gbaguidi G, Fruchart JC and Staels B: Pleiotropic effects of fibrates. Curr Atheroscler Rep 7: 396-401, 2005.
4. Jun M, Foote C, Lv J, Neal B, Patel A, Nicholls SJ, Grobbee DE, Cass A, Chalmers J and Perkovic V: Effects of fibrates on cardiovascular outcomes: A systematic review and meta-analysis. Lancet 375: 1875-1884, 2010.
5. Keech A, Simes RJ, Barter P, Best J, Scott R, Taskinen MR, Forder P, Pillai A, Davis T, Glasziou P, *et al*: Effects of long-term fenofibrate therapy on cardiovascular events in 9,795 people with type 2 diabetes mellitus (the FIELD study): Randomised controlled trial. Lancet 366: 1849-1861, 2005.
6. Kleiner DE, Brunt EM, Van Natta M, Behling C, Contos MJ, Cummings OW, Ferrell LD, Liu YC, Torbenson MS, Unalp-Arida A, *et al*: Design and validation of a histological scoring system for nonalcoholic fatty liver disease. Hepatology 41: 1313-1321, 2005.
7. Brunt EM: Pathology of nonalcoholic fatty liver disease. Nat Rev Gastroenterol Hepatol 7: 195-203, 2010.
8. Ajmal MR, Yaccha M, Malik MA, Rabbani MU, Ahmad I, Isalm N and Abdali N: Prevalence of nonalcoholic fatty liver disease (NAFLD) in patients of cardiovascular diseases and its association with hs-CRP and TNF-α. Indian Heart J 66: 574-579, 2014.
9. Narasimhan S, Gokulakrishnan K, Sampathkumar R, Farooq S, Ravikumar R, Mohan V and Balasubramanyam M: Oxidative stress is independently associated with non-alcoholic fatty liver disease (NAFLD) in subjects with and without type 2 diabetes. Clin Biochem 43: 815-821, 2010.
10. Duan XY, Zhang L, Fan JG and Qiao L: NAFLD leads to liver cancer: Do we have sufficient evidence? Cancer Lett 345: 230-234, 2014.
11. Shifflet A and Wu YG: Non-alcoholic steatohepatitis: An overview. J Formos Med Assoc 108: 4-12, 2009.
12. Day CP and James OF: Steatohepatitis: A tale of two 'hits'? Gastroenterology 114: 842-845, 1998.
13. Musso G, Gambino R and Cassader M: Recent insights into hepatic lipid metabolism in non-alcoholic fatty liver disease (NAFLD). Prog Lipid Res 48: 1-26, 2009.
14. Cui W, Chen SL and Hu KQ: Quantification and mechanisms of oleic acidinduced steatosis in HepG2 cells. Am J Transl Res 2: 95-104, 2010.
15. Wang S, Kuang X, Fang ZJ, Huang Z and Shi P: Effect of oleic acid on the levels of eight metal ions in human hepatoma SMMC-7721 cells. Biol Trace Elem Res 159: 445-450, 2014.
16. Ramírez-Zacarías JL, Castro-Muñozledo F and Kuri-Harcuch W: Quantitation of adipose conversion and triglycerides by staining intracytoplasmic lipids with Oil red O. Histochemistry 6: 493-497, 1992.
17. Bergman AC, Benjamin T, Alaiya A, Waltham M, Sakaguchi K, Franzén B, Linder S, Bergman T, Auer G, Appella E, *et al*: Identification of gel-separated tumor marker proteins by mass spectrometry. Electrophoresis 21: 679-686, 2000.
18. Livak KJ and Schmittgen TD: Analysis of relative gene expression data using real-time quantitative PCR and the 2(-Delta Delta C(T)) method. Methods 25: 402-408, 2001.
19. Bradford MM: A rapid and sensitive method for quantitation of microgram quantities of protein utilizing the principle of protein-dye binding. Anal Biochem 72: 248-254, 1976.
20. Brown MS and Goldstein JL: The SREBP pathway: Regulation of cholesterol metabolism by proteolysis of a membrane-bound transcription factor. Cell 89: 331-340, 1997.
21. Huang H, McIntosh AL, Martin AG, Petrescu AD, Landrock KK, Landrock D, Kier AB and Schroeder F: Inhibitors of fatty acid synthesis induce PPAR α-regulated fatty acid β-oxidative genes: Synergistic roles of L-FABP and glucose. PPAR Res 2013: 804-865, 2013.
22. Bishop-Bailey D: Peroxisome proliferator-activated receptors in the cardiovascular system. Br J Pharmacol 129: 823-834, 2000.
23. Smith WJ, Wang J, Dang AQ, Reeves C, Bibbs D and Faas FH: Gemfibrozil lowers plasma lipids and increases polyunsaturated fatty acid content and oxidative susceptibility of lipoproteins in hypertriglyceridemia. Clin Chim Acta 322: 77-84, 2002.
24. Uchida A, Slipchenko MN, Cheng JX and Buhman KK: Fenofibrate, a peroxisome proliferator-activated receptor α agonist, alters triglyceride metabolism in enterocytes of mice. Biochim Biophys Acta 1811: 170-176, 2011.
25. Peters JM, Rusyn I, Rose ML, Gonzalez FJ and Thurman RG: Peroxisome proliferator-activated receptor alpha is restricted to hepatic parenchymal cells, not Kupffer cells: Implications for the mechanism of action of peroxisome proliferators in hepatocarcinogenesis. Carcinogenesis 21: 823-826, 2000.
26. Fernández-Rojo MA, Restall C, Ferguson C, Martel N, Martin S, Bosch M, Kassan A, Leong GM, Martin SD, McGee SL, *et al*: Caveolin-1 orchestrates the balance between glucose and lipid-dependent energy metabolism: Implications for liver regeneration. Hepatology 55: 1574-1584, 2012.

27. Ogata M, Tsujita M, Hossaina MA, Akita N, Gonzalez FJ, Staels B, Suzuki S, Fukutomi T, Kimura G and Yokoyama S: On the mechanism for PPAR agonists to enhance ABCA1 gene expression. Atherosclerosis 205: 413-419, 2009.
28. Mimeault C, Trudeau VL and Moon TW: Waterborne gemfibrozil challenges the hepatic antioxidant defense system and down-regulates peroxisome proliferator activated receptor beta (PPARbeta) mRNA levels in male goldfish (Carassius auratus). Toxicology 228: 140-150, 2006.
29. Passeri MJ, Cinaroglu A, Gao C and Sadler KC: Hepatic steatosis in response to acute alcohol exposure in zebrafish requires sterol regulatory element binding protein activation. Hepatology 49: 443-452, 2009.
30. Li W, Tai Y, Zhou J, Gu W, Bai Z, Zhou T, Zhong Z, McCue PA, Sang N, Ji JY, *et al*: Repression of endometrial tumor growth by targeting SREBP1 and lipogenesis. Cell Cycle 11: 2348-2358, 2012.
31. Stone SJ, Myers HM, Watkins SM, Brown BE, Feingold KR, Elias PM and Farese RV Jr: Lipopenia and skin barrier abnormalities in DGAT2-deficient mice. J Biol Chem 279: 11767-11776, 2004.
32. Sumida Y, Niki E, Naito Y and Yoshikawa: Involvement of free radicals and oxidative stress in NAFLD/NASH. Free Radical Res 47: 869-880, 2004.
33. Horton JD, Bashmakov Y, Shimomura I and Shimano H: Regulation of sterol regulatory element binding proteins in livers of fasted and refed mice. Proc Natl Acad Sci USA 95: 5987-5992, 1998.
34. Kok BP, Dyck JR, Harris TE and Brindley DN: Differential regulation of the expressions of the PGC-1α splice variants, lipins, and PPARα in heart compared to liver. J Lipid Res 54: 1662-1677, 2013.
35. Péterfy M, Phan J, Xu P and Reue K: Lipodystrophy in the fld mouse results from mutation of a new gene encoding a nuclear protein. Lipin Nat Genet 27: 121-124, 2001.
36. Yen CLE, Stone SJ, Koliwad S, Harris C and Farese RV Jr: Thematic review series: Glycerolipids. DGAT enzymes and triacylglycerol biosynthesis. J Lipid Res 49: 2283-2301, 2008.
37. Li C, Li L, Lian J, Watts R, Nelson R, Goodwin B and Lehner R: Roles of Acyl-CoA: Diacylglycerol acyltransferases 1 and 2 in triacylglycerol synthesis and secretion in primary hepatocytes. Arterioscl Throm Vas 35: 1080-1091, 2015.
38. Ibrahimi A and Abumrad NA: Role of CD36 in membrane transport of long-chain fatty acids. Curr Opin Clin Nutr 5: 139-145, 2002.
39. Kennedy DJ, Kuchibhotla S, Westfall KM, Silverstein RL, Morton RE and Febbraio M: A CD36-dependent pathway enhances macrophage and adipose tissue inflammation and impairs insulin signalling. Cardiovasc Res 89: 604-613, 2011.
40. Ouwens DM, Diamant M, Fodor M, Habets DDJ, Pelsers MMAL, El Hasnaoui M, Dang ZC, van den Brom CE, Vlasblom R, Rietdijk A, *et al*: Cardiac contractile dysfunction in insulin-resistant rats fed a high-fat diet is associated with elevated CD36-mediated fatty acid uptake and esterification. Diabetologia 50: 1938-1948, 2007.
41. Koonen DP, Jacobs RL, Febbraio M, Young ME, Soltys CL, Ong H, Vance DE and Dyck JR: Increased hepatic CD36 expression contributes to dyslipidemia associated with diet-induced obesity. Diabetes 56: 2863-2871, 2007.
42. Miquilena-Colina ME, Lima-Cabello E, Sánchez-Campos S, García-Mediavilla MV, Fernández-Bermejo M, Lozano-Rodríguez T, Vargas-Castrillón J, Buqué X, Ochoa B, Aspichueta P, *et al*: Hepatic fatty acid translocase CD36 upregulation is associated with insulin resistance, hyperinsulinaemia and increased steatosis in non-alcoholic steatohepatitis and chronic hepatitis C. Gut 60: 1394-1402, 2011.